

Scientific Review – Engineering and Environmental Sciences (2018), 27 (4), 410–424  
Sci. Rev. Eng. Env. Sci. (2018), 27 (4)  
Przegląd Naukowy – Inżynieria i Kształtowanie Środowiska (2018), 27 (4), 410–424  
Prz. Nauk. Inż. Kszt. Środ. (2018), 27 (4)  
<http://iks.pn.sggw.pl>  
DOI 10.22630/PNIKS.2018.27.4.40

**Moses E. EMETERE<sup>1,2</sup>, Samuel E. SANNI<sup>3</sup>, Emmanuel E. OKORO<sup>3</sup>,  
Gideon A. ADEYEMI<sup>1</sup>**

<sup>1,2</sup>College of Science and Technology, Covenant University Canaan land

<sup>2</sup>School of Mechanical Engineering and Science, University of Johannesburg

<sup>3</sup>College of Engineering, Covenant University

## **Aerosol loading and its effect on respiratory dysfunction disorder over Dapaong-Togo**

**Key words:** air pollution, aerosol, Dapaong, respiratory, model

### **Introduction**

Atmospheric aerosols (AA) is dangerous to human health when the emission rate is presumably high. The water-soluble part of atmospheric aerosol particle originates from gas to particle conversion and consists of various kinds of sulphates, nitrates, organic and water-soluble substances. The soot is made-up of incombustible black carbon. Mineral aerosol or desert dust consists of a mixture of quartz and clay minerals. Antarctic aerosol or sulphate aerosol consists of a large amount of sulphate, that is, 75% H<sub>2</sub>SO<sub>4</sub>. When AA is inhaled in large volume/quantity, it deposits in the lungs and undergoes chemical changes, particularly when passing through the

lungs to other sensitive organs of the body. Hence, aside respiratory dysfunction, inhalation of atmospheric aerosols may lead to cancer, arrhythmias, atrial fibrillation, acute coronary syndromes, cardiovasculer malfunction etc.

The science of the aerosol transport through the lungs is known (Newman, Clark, Talaee & Clarke, 1989; Hofmann & Koblinger, 1992; Edwards, 1995; Goikoetxea et al., 2014) as well as the peculiarity of aerosol loading over West Africa (Emetere, Akinyemi & Akinojo, 2015; Emetere 2016a, b, c) where the research site is located. In this study, we are interested in documenting numerical values of the current state of aerosol loading into the atmosphere, its sizes and the deposition efficiency of the atmospheric aerosols into human lungs. This information is very vital for furture work over Dapaong-Togo.

## Experimental design, materials and methods

Dapaong is located on latitude 10.8733° N and longitude 0.2010° E as shown on the Google map (Fig. 1). The primary data was obtained from Multi-angle Imaging Spectro-Radiometer (MISR). The aerosol retention and loading were obtained using the West African regional scale dispersion model (WASDM). This model has been proven to be reliable for calculating aerosol loading over the West African region. It is mathematically given as (Emetere, 2016b):

$$\psi(\lambda) = a_1^2 \cos\left(\frac{n_1\pi\tau(\lambda)}{2}x\right) \cos\left(\frac{n_1\pi\tau(\lambda)}{2}y\right) + \dots \\ \dots + a_n^2 \cos\left(\frac{n_n\pi\tau(\lambda)}{2}x\right) \cos\left(\frac{n_n\pi\tau(\lambda)}{2}y\right) \quad (1)$$

$a$  is atmospheric constant gotten from the fifteen years aerosol optical depth (AOD) dataset from MISR,  $n$  is the tuning constant,  $\tau^{(\lambda)}$  is the AOD of the area and  $\psi^{(\lambda)}$  is the aerosol loading.

The digital voltage and Angstrom parameters of the study area can be obtained from Equations (2) and (3) respectively.

$$I(555) = \frac{I_o(555)}{R^2} \exp[m \cdot \tau(555)] \quad (2)$$

where  $I$  is the solar radiance over the SPM detector at wavelength  $\lambda = 555$  nm,  $I_o$  is the measure of solar radiation behind the atmosphere,  $R$  is the mean Earth–Sun distance in astronomical units,  $\tau$  is the total optical depth (in this case, the average of the each month is referred to as the total AOD, and  $m$  is the optical air mass.

$$\alpha = -\frac{d \ln(\tau)}{d \ln(\lambda)} \quad (3)$$



FIGURE 1. Google map over Dapaong

where  $\alpha$  is the Angstrom parameter,  $\tau$  is the aerosol optical depth, and  $\lambda$  is the wavelength. The radius of the particles for atmospheric aerosol was calculated using proposals by Kokhanovsky et al. (2006). The analysis of Equations (1–3) was done using the C++ codes, Surfer software and Excel.

The aerosols deposition into the human lungs (Fig. 2) has been modelled as documented in Martonen and Zhang (1992), Darquenne and Kin (2004), Varughese and Gangamma (2006), Goikote et al. (2014) and Ching and Kajino (2018).

$$\eta = [1 - \exp(-39.9Q^{0.14}D^{0.599})] + \\ + \{1 + \exp[12.39 - 2.92 \log(\rho D_p^2 Q)]\}^{-1} \quad (4)$$

where  $\eta$  is the deposition efficiency,  $Q$  volumetric flow rate,  $D$  is the diffusion

coefficient of the particle,  $D_p$  is the particle density and  $\rho$  is the particle diameter.

The flowchart that summarized the methodology adopted to execute this research work is highlighted in Figure 3.

## Results and discussion

Aerosol loading parameters are shown in Figures 4 and 5. The aerosol loading is high and almost constant at about 0.96 throughout fourteen years. This is an evidence that the source of the aerosol loading is sustainably influencing the risk of human to respiratory dysfunction. From literature, the sources of pollution is Sahara dust and anthropogenic pollution. The anthropogenic pollution may be inferred from the Google map presented in Figure 1. The anthropogenic sources include bush burning, automobile gas emission, domestic fuel burning

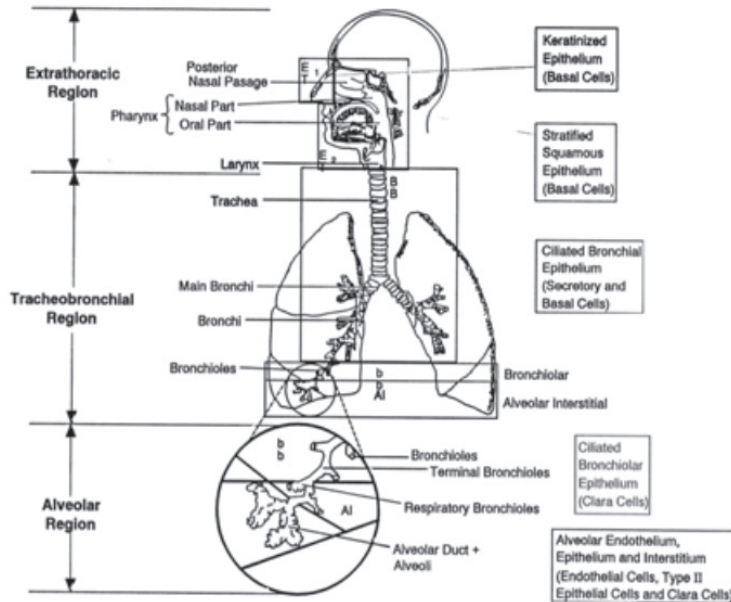


FIGURE 2. The respiratory component of the human being (Hofmann and Koblinger, 1992)

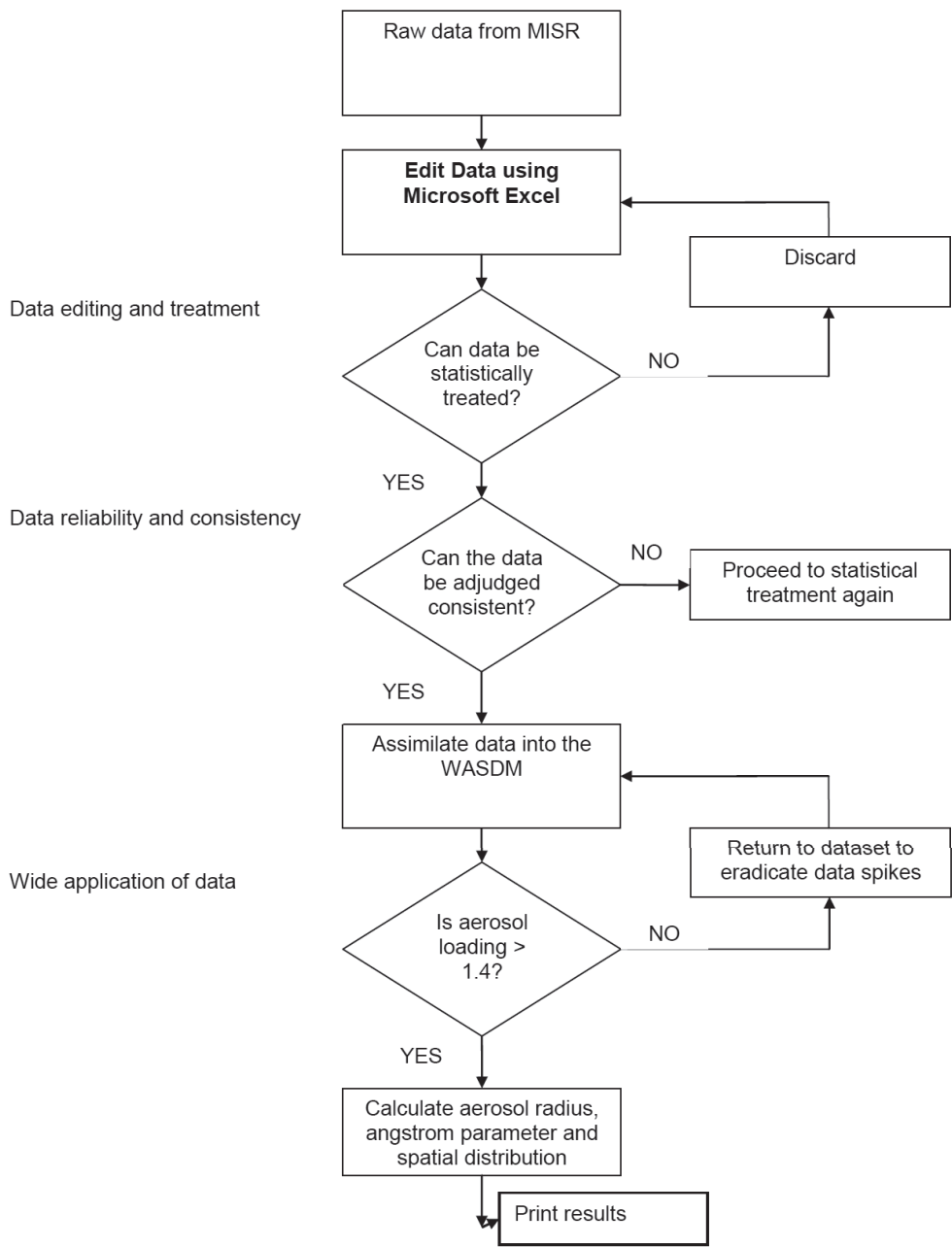


FIGURE 3. Flowchart of the research methodology

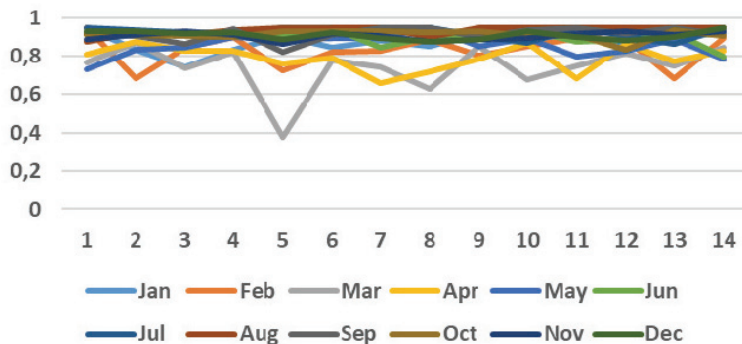


FIGURE 4. Aerosol loading versus years (2000–2013)

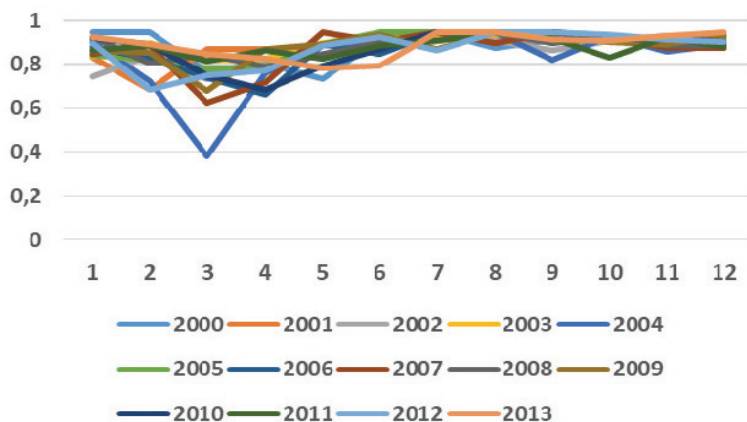


FIGURE 5. Aerosol loading versus month of year (2000–2013)

(e.g. fire wood, charcoal, kerosene etc.) and industrial emission. In Figure 4, the highest aerosol loading for fourteen years was found to occur in March 2004. However, in 2013, the highest aerosol loading was found to be in the month of May. This may be due to climate change and it is an evidence of a dismal rainfall pattern over the area. In Figure 5, it was observed that the transient nature of the aerosol loading over the research area was between January and May. This result partly shows the period where Sahara dust flow is highest. The dominant pollutant can be traced from the Angstrom exponent, which describes

the dependency of the aerosol optical thickness or aerosol extinction coefficient on wavelength. So when the Angstrom exponent is  $< 0.1$ , the aerosols is likely black carbon, when the Angstrom exponent is  $> 0.1$ , the aerosols is a mixture of black carbon, dust and unknown pollutants. The lowest aerosol loading ever recorded was in March 2005 (Figs. 6 and 7). Over two decades, the aerosol loading is lowest between February and May while the highest aerosol loading is between June and January. It has been proven that precipitation rate lowers the aerosol loading in the atmosphere (Emetere, 2016a). The ANOVA of the aerosol

loading is presented in Table 1. The coefficient of multiple determination is given as 0.35988. The result in Table 1 further show that the source of the pollution is sustainable over fifteen years.

Some scientists have shown that the sizes of pollutants determine the danger that maybe encountered during inhalation of atmospheric aerosols. For example, Yu and Xu (1987) and Ching and Kajino (2018) worked on the regional and total deposition of 200 nm particles in the lungs of children and adult. It was observed that the total deposition in the tracheo-bronchial has risen by a factor of 20% in children relative to adults. This ascertainment was experimentally validated by Bequemin, Yu, Roy and Bouchikhi (1990) and Schiller-Scotland, Hlawa, Gebhardt, Wönnne and Heyder (1992). This was the motivation for the estima-

tion of the aerosol/particulate radius over Dapaong. The aerosol radius fluctuated all through fifteen years (Fig. 6). The largest aerosol radius was found in March 2005 when the aerosol loading is presumably low. It leads to the first hypothesis that low aerosol loading indicates that the sizes of the aerosols is large. Hence at high aerosol loading, the aerosol radius is very small to penetrate the nostrils into the lungs. In the research area, soot from anthropogenic sources is more and visible via its deposition on surfaces of leaves and roofs. The coefficient of multiple determination is given as 0.445. The ANOVA shown in Table 2 depicts that the aerosol radius is presumably low to affect respiratory process in human.

In Figures 8–10, we show the spatial distribution of aerosol optical depth, aer-

TABLE 1. ANOVA for aerosol loading at coefficient of multiple determination,  $R^2 = 0.35987994954612$

Source	<i>df</i>	SS	MS	<i>F</i>
Regression	2	0.0176	0.0088	2.5299
Residual	9	0.0313	0.0034	×
Total	11	0.0489	×	×

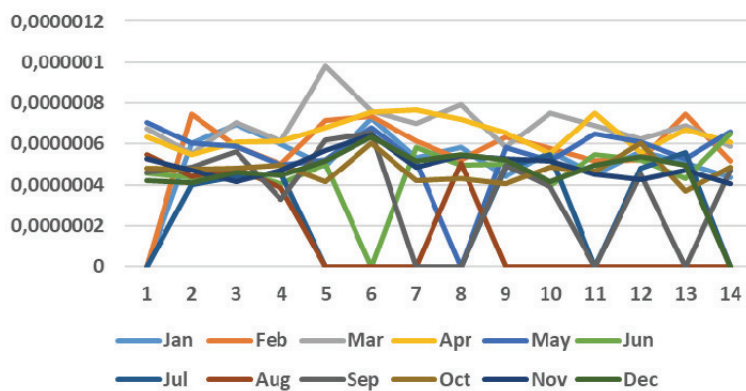


FIGURE 6. Atmospheric aerosol radius versus month of year (2000–2013)

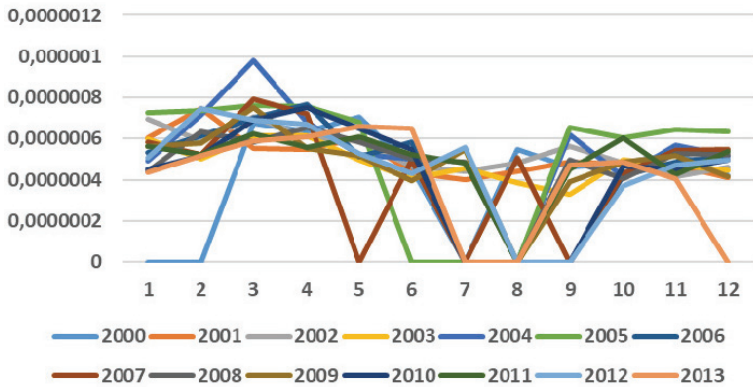


FIGURE 7. Atmospheric aerosol radius versus month of year (2000–2013)

TABLE 2. ANOVA for aerosol radius at coefficient of multiple determination  $R^2 = 0.44999742735105$

Source	<i>df</i>	<i>SS</i>	<i>MS</i>	<i>F</i>
Regression	2	3.5373E-014	1.7686E-014	3.6818
Residual	9	4.3234E-014	4.8038E-015	×
Total	11	7.8608E-014	×	×

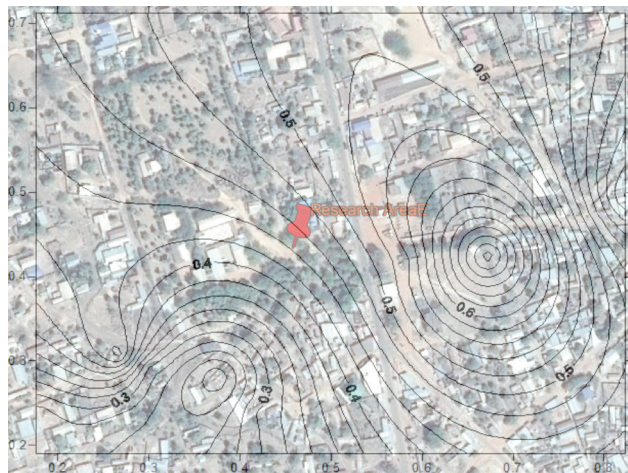


FIGURE 8. Spatial distribution of aerosol optical depth. Map scale 1 : 200 000

osol loading and aerosol radius. The aerosol optical depth distribution reveals that the main pollution source in Dapaong is the agrarian area (Fig. 8). The Angstrom exponent over Dapaong is shown in Ta-

bles 3, 4 and 5. The statistical analysis of the AOD dataset obtained from MISR is shown in Tables 6, 7 and 8. This statistical values (i.e. number of values, number of missing values, minimum, maximum,



FIGURE 9. Spatial distribution of aerosol loading depth. Map scale 1 : 200 000

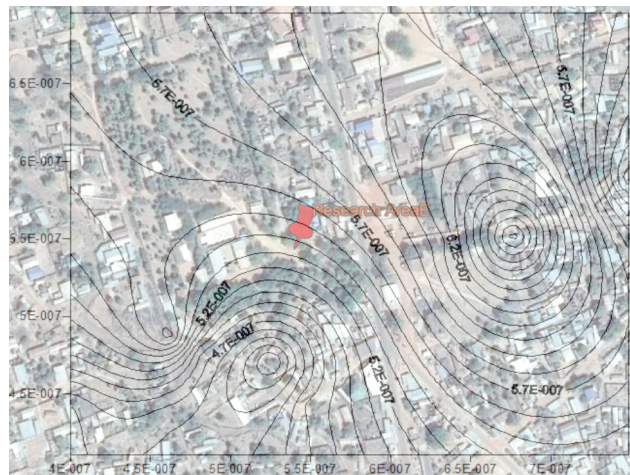


FIGURE 10. Spatial distribution of aerosol radius [m]. Map scale 1 : 200 000

mean, first quartile, third quartile, standard error, 95% confidence interval, 99% confidence interval, variance, average deviation, standard deviation, coefficient of variation, skew, kurtosis, Kolmogorov–Smirnov, critical K-S stat for 0.1, 0.05 and 0.01) give insight on the reliability of remote sensing techniques in aiding the present research. The average and standard deviation are considerable low

and consistent. The standard error show that the dataset is very reliable in taking a confident conclusion. Due to forces of wind and advection, the aerosol loading shifts in the opposite direction (Emetere, 2016) where there is human settlement (north-east of Fig. 9). Like the AOD, the spatial distribution of the aerosols radius is in tandem to the pollution sources (Fig. 10). Hence, it is confirmed from

TABLE 3. Angstrom exponent over Dapaong

Month	2000	2001	2002	2003	2004
Jan	#NUM!	0.10295458	0.0537552	0.1037909	0.18348319
Feb	#NUM!	0.03082767	0.11117707	0.17259845	0.044895
March	0.062905356	0.13578512	0.04915511	0.09518643	-0.0441758
April	0.085117425	0.13747367	0.09883803	0.09702604	0.06002723
May	0.048508737	0.10197187	0.1113902	0.17617092	0.15649097
June	0.213179371	0.23361711	0.20545815	0.26703718	0.17449373
July	#NUM!	0.27492959	0.22985306	0.21257187	#NUM!
Aug	0.139180439	0.22717073	0.19159169	0.2930082	#NUM!
Sep	0.208383438	0.18688297	0.1270717	0.37418459	0.09204126
Oct	0.192123638	0.19535342	0.19053313	0.17900636	0.25689057
Nov	0.154938755	0.20051232	0.25443595	0.20131028	0.1249663
Dec	0.250534672	0.26219338	0.20823588	0.22388052	0.15928059

TABLE 4. Angstrom exponent over Dapaong

Month	2005	2006	2007	2008	2009
Jan	0.10937691	0.14914834	0.11549531	0.23166688	0.12786851
Feb	0.09446611	0.09663697	0.15606612	0.08376828	0.11714552
March	0.0679297	0.05165763	0.01285179	0.11557741	0.02891637
April	0.0757786	0.02276802	0.04246188	0.07355902	0.13541232
May	0.16094911	0.16674224	#NUM!	0.11516732	0.16146043
June	#NUM!	0.11369973	0.17835377	0.17165926	0.2804187
July	#NUM!	#NUM!	#NUM!	0.18688297	0.13690882
Aug	#NUM!	#NUM!	0.16979743	#NUM!	#NUM!
Sep	0.19159169	#NUM!	#NUM!	0.17568991	0.28466421
Oct	0.26449149	0.25234331	0.23985626	0.27049642	0.18636832
Nov	0.20858039	0.1873993	0.14161417	0.15229301	0.16109503
Dec	0.22339283	0.16014893	0.14013666	0.15820183	0.25682373

the above (Tables 1–4 and Figs. 4–10) that the main source of pollution over Dapaong is from anthropogenic source (June to December) and Sahara dust (January to May).

The last section focus on how this atmospheric aerosol affects human population in Dapaong. The deposition efficiency was estimated using Equation (4). The  $D_p$

was substitute with the aerosol radius that was calculated in Figure 6. It is observed in Figure 11 that the highest deposition efficiency into human lungs occurred in 2000 and 2001. However, it has been very consistent in eleven years. The consistent value of the deposition efficiency is 0.955. If an assumption is made that the deposition efficiency over Dapaong between

TABLE 5. Angstrom exponent over Dapaong

Month	2010	2011	2012	2013
Jan	0.22065731	0.12671885	0.16738655	0.23292604
Feb	0.16168008	0.15564242	0.03057149	0.16109503
March	0.0553936	0.0893744	0.05524395	0.11213845
April	0.03044356	0.12980336	0.06599681	0.09846906
May	0.07727581	0.09780706	0.15312374	0.0711219
June	0.13766241	0.15663283	0.23818413	0.07744783
July	#NUM!	0.19053313	0.12974347	#NUM!
Aug	#NUM!	#NUM!	#NUM!	#NUM!
Sep	#NUM!	0.21875444	#NUM!	0.19892837
Oct	0.204591	0.10287877	0.31114461	0.18791731
Nov	0.21729009	0.24547821	0.20060599	0.26639691
Dec	0.17884296	0.14629745	0.1776228	#NUM!

TABLE 6. AOD statistics over Dapaong

Statistics	2000	2001	2002	2003	2004
Number of values	9.0000	12.0000	12.0000	12.0000	10.0000
Number of missing values	3.0000	0	0	0	2
Minimum	0.2053	0.176	0.200333333	0.094	0.19725
Maximum	0.736	0.823	0.733	0.548	1.322
Mean	0.42366666	0.368847222	0.416006944	0.318006944	0.535275
First quartile	0.266	0.23325	0.270625	0.214	0.332
Third quartile	0.606	0.472875	0.515416667	0.4275	0.684333333
Standard error	0.06476884	0.053854318	0.052598151	0.043333526	0.103058853
95% confidence interval	0.1493569	0.118533353	0.11576853	0.09537709	0.233119125
99% confidence interval	0.2172994	0.167271511	0.163369857	0.134593931	0.334941272
Variance	0.0377550	0.034803451	0.033198786	0.022533533	0.106211272
Average deviation	0.1602222	0.144835648	0.153743056	0.114631944	0.235446667
Standard deviation	0.1943065	0.186556829	0.18220534	0.150111736	0.325900708
Coefficient of variation	0.45863	0.50578	0.43799	0.47204	0.60885
Skew	0.64	1.38	0.633	0.421	1.737
Kurtosis	-1.223	2.065	-0.804	-0.781	3.488
Kolmogorov-Smirnov stat	0.187	0.213	0.238	0.203	0.198

TABLE 6, cont.

Statistics	2000	2001	2002	2003	2004
Critical K-S stat, $\alpha = 0.10$	0.387	0.338	0.338	0.338	0.369
Critical K-S stat, $\alpha = 0.05$	0.43	0.375	0.375	0.375	0.409
Critical K-S stat, $\alpha = 0.01$	0.513	0.449	0.449	0.449	0.489

TABLE 7. AOD statistics over Dapaong

Statistics	2005	2006	2007	2008	2009
Number of values	9.0000	9.0000	9.0000	11.0000	11.0000
Number of missing values	3.0000	3.0000	3.0000	1.0000	1.0000
Minimum	0.1880	0.2030	0.2197	0.1810	0.1655
Maximum	0.6510	0.8660	0.9220	0.6283	0.8330
Mean	0.4090	0.4699	0.4721	0.3926	0.3786
First quartile	0.2617	0.3380	0.3375	0.3126	0.2250
Third quartile	0.5678	0.5876	0.5527	0.4827	0.4406
Standard error	0.0579	0.0703	0.0752	0.0422	0.0566
95% confidence interval	0.1337	0.1622	0.1736	0.0941	0.1260
99% confidence interval	0.1945	0.2361	0.2526	0.13378	0.1793
Variance	0.0303	0.04456	0.0510	0.0196	0.0352
Average deviation	0.1524	0.1641	0.1672	0.1112	0.1289
Standard deviation	0.1739	0.2111	0.2259	0.1400	0.1876
Coefficient of variation	0.4253	0.4492	0.4785	0.3566	0.4956
Skew	0.2290	0.8820	1.3000	0.3280	1.2990
Kurtosis	-1.7760	0.1300	0.9120	-0.6070	2.9080
Kolmogorov–Smirnov stat	0.1830	0.2040	0.2710	0.1660	0.2090
Critical K-S stat, $\alpha = 0.10$	0.3870	0.3870	0.3870	0.3520	0.3520
Critical K-S stat, $\alpha = 0.05$	0.4300	0.4300	0.4300	0.3910	0.3910
Critical K-S stat, $\alpha = 0.01$	0.5130	0.5130	0.5130	0.4680	0.4680

TABLE 8. AOD statistics over Dapaong

Statistics	2010	2011	2012	2013
Number of values	9	11	10	9
Number of missing values	3	1	2	3
Minimum	0.248	0.212	0.14	0.18575
Maximum	0.825	0.5685	0.824333333	0.638
Mean	0.446796296	0.402204545	0.432541667	0.40512963
First quartile	0.269208333	0.317916667	0.2815	0.27075
Third quartile	0.636416667	0.50375	0.659	0.5558125
Standard error	0.071457694	0.035110981	0.070983404	0.056252884
95% confidence interval	0.164781442	0.078227265	0.160564461	0.129719151
99% confidence interval	0.239740562	0.111266698	0.230696065	0.188728427
Variance	0.045955818	0.013560591	0.050386437	0.028479483
Average deviation	0.178432099	0.092329201	0.1798	0.146569959
Standard deviation	0.214373081	0.11644995	0.224469234	0.168758653
Coefficient of variation	0.4798	0.28953	0.51895	0.41655
Skew	0.866	-0.187	0.642	0.192
Kurtosis	-0.793	-0.907	-0.752	-1.682
Kolmogorov-Smirnov stat	0.218	0.124	0.192	0.168
Critical K-S stat, $\alpha = 0.10$	0.387	0.352	0.369	0.387
Critical K-S stat, $\alpha = 0.05$	0.43	0.391	0.409	0.43
Critical K-S stat, $\alpha = 0.01$	0.513	0.468	0.489	0.513

2002–2018 is true, then the report given by Borgen project (Borgen, 2018) that 20% of deaths in Togo is caused by respiratory diseases can be adjudged as very true.

## Conclusions

Through a systematic investigation, it was affirmed that the main source of pollution over Dapaong is bush and do-

mestic fuel burning (June to December) and Sahara dust (January to May). It was observed that the sources of pollution have been very consistent over two decades. The largest aerosol radius was found when the aerosol loading is presumably low. Hence, at high aerosol loading, the aerosol radius is very small to penetrate the nostrils into the lungs. The depositional efficiency of aerosols

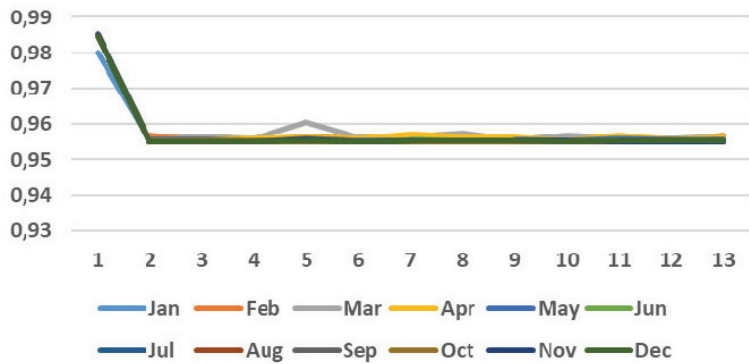


FIGURE 11. Deposition efficiency in human lungs versus year

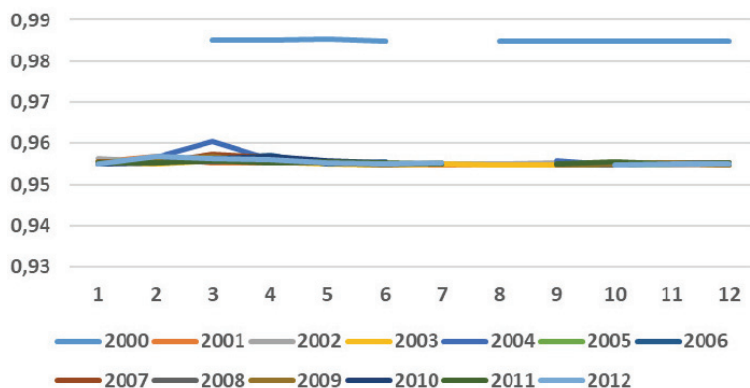


FIGURE 12. Deposition efficiency in human lungs versus month of year (2000–2013)

was estimated as 0,955. If an assumption is made that the deposition efficiency over Dapaong between 2002–2018 is true, then the report given by Borgen project (that 20% of deaths in Togo is caused by respiratory diseases) may be adjudged as very true.

## Acknowledgements

The authors appreciate Covenant University for partial sponsorship. The authors acknowledge NASA for primary dataset. The authors declare that there is

no conflict of interest for this research. M.E. Emetere enjoys partial sponsorship as a Senior Research Associate at University of Johannesburg.

## References

- Bequemin, M.H., Yu, C.P., Roy, M. & Bouchikhi, A.(1990). Total deposition of inhaled particles related to age: comparison with age dependent model calculations. *Third International Workshop on Respiratory Tract Dosimetry*, 1-3 July, Albuquerque, New Mexico.
- Borgen (2018). *Common diseases in Togo*. Retrieved from: <https://borgenproject.org/common-diseases-in-togo/>

- mon-diseases-in-togo/ (accessed: 30.07. 2018).
- Ching, J. & Kajino, M. (2018). Aerosol mixing state matters for particles deposition in human respiratory system. *Scientific Reports*, 8, 8864.
- Edwards, D.A. (1995). The macrotransport of aerosol particles in the lung: Aerosol deposition phenomena. *Journal of Aerosol Science*, 26(2), 293-317.
- Emetere, M.E. (2016a). *Numerical modelling of west africa regional scale aerosol dispersion*. (a doctoral thesis). Ota: Covenant University.
- Emetere, M.E. (2016b). Generation Of Atmospheric Constants Over Some Locations In West Africa: A Theoretical Aid for Measuring Instruments Design. *International Journal of Engineering Research in Africa*, 27, 119-146.
- Emetere, M.E. (2016c). Statistical Examination of the Aerosols Loading Over Mubi-Nigeria: The Satellite Observation Analysis. *Geographica Panonica*, 20(1), 42-50.
- Emetere, M.E., Akinyemi, M.L., & Akinojo O. (2015) Parametric retrieval model for estimating aerosol size distribution via the AERONET, LAGOS station. *Environmental Pollution*, 207(C), 381-390.
- Darquenne, C. & Kin Prisk G. (2004). Aerosol Deposition in the Human Respiratory Tract Breathing Air and 80:20 Heliox. *Journal of Aerosol Medicine*, 17(3), 278-285.
- Goikoetxea, E., Murgia, X., Serna-Grande, P., Valls-i-Soler, A., Rey-Santano, C., Rivas, A., ... & Lopez-Arraiza, A. (2014). In vitro surfactant and perfluorocarbon aerosol deposition in a neonatal physical model of the upper conducting airways. *PLOS ONE*, 9(9), e106835.
- Hofmann, W. & Koblinger, L. (1992). Monte Carlo modeling of aerosol deposition in human lungs. Part III: Comparison with experimental data. *Journal of Aerosol Science*, 23(1), 51-63.
- Jakobsson, J.K., Hedlund, J., Kumlin, J., Wollmer, P. & Löndahl, J. (2016). A new method for measuring lung deposition efficiency of airborne nanoparticles in a single breath. *Scientific Reports*, 6, 36147.
- Kokhanovsky, A.A., von Hoyningen-Huene, W. & Burrows, J.P. (2006). Atmospheric aerosol load as derived from space. *Atmospheric Research*, 81, 176-185.
- Martonen, T.B. & Zhang, (1992). Comments on recent Data for Particle Deposition in Human Nasal Passages. *Journal of Aerosol Science*, 23, 667-674.
- Newman, S.P., Clark, A.R., Talaee, N. & Clarke, S.W. (1989). Pressurised aerosol deposition in the human lung with and without an "open" spacer device. *Thorax*, 44, 706-710.
- Schiller-Scotland, Ch.F., Hlawa, R., Gebhardt, J., Wönnne, R. & Heyder, J. (1992). Total deposition of aerosol particles in the respiratory tracts of children during spontaneous and controlled mouth breathing. *Journal of Aerosol Science*, 23, S457-S460.
- Varghese Suresh, K. & Gangamma, S. (2006). Particle Deposition in Human Respiratory Tract: Effect of Water-Soluble Fraction. *Aerosol and Air Quality Research*, 6(4), 360-379.
- Yu, C.P. & Xu, G.B., (1987). Predicted deposition of diesel particles in young humans. *Journal of Aerosol Science*, 18, 419-430.

## Summary

**Aerosol loading and its effect on respiratory dysfunction disorder over Dapaong-Togo.** It has been reported that respiratory dysfunction is responsible for 20% of deaths in Togo. There is need to know (in numerical value) the current state and future prediction of aerosol loading over the research site. The research is based on remote sensing techniques and proven mathematical models. Fifteen years primary (aerosol optical depth) dataset was obtained from the Multi-angle Imaging Spectro-Radiometer (MISR). The secondary datasets (aerosol loading, particles sizes, Angstrom exponent and the statistics of the primary dataset) was generated from the primary data. The average deposition efficiency of aerosols (into the human lungs) in the region is about 0.955. This research provides vital data for health referencing and on-ground investigation over Dapaong-Togo.

**Authors' address:**

Moses Emetere  
Covenant University  
Department of Physics  
Canaan land, P.M.B 1023, Ota  
Nigeria  
e-mail: moses.emetere@covenantuniversity.edu.ng